Journal of Molecular Structure 1002 (2011) 135–144

Contents lists available at ScienceDirect

Journal of Molecular Structure

journal homepage: www.elsevier.com/locate/molstruc

Synthesis and properties of copper (II), oxovanadium (IV) and gadolinium (III) complexes derived from polar Schiff's bases

Lopamudra Chakraborty, Nirmalangshu Chakraborty, Atiqur Rahman Laskar, Manoj Kumar Paul, Nandiraju V.S. Rao *

Chemistry Department, Assam University, Silchar 788 011, Assam, India

ARTICLE INFO

Article history:
Received 1 April 2011
Received in revised form 5 July 2011
Accepted 5 July 2011
Available online 10 August 2011

Keywords:
Metallomesogens
Liquid crystals
Smectic phase
Polar compounds
Schiff's bases

ABSTRACT

The synthesis, liquid crystalline and optical properties of copper (II), oxovanadium (IV) and gadolinium (III) complexes derived from polar Schiff's bases viz., N-(4-n-hexadecyloxysalicylidene)-4′-substituted anilines with methoxy, fluoro and chloro substituents in the 4-position of N-aryl moiety are presented. All the ligands exhibited smectic A phase except methoxy homolog which exhibited nematic phase. Majority of the complexes exhibited smectic A phase with some of them exhibiting smectic E phases. The UV–Visible and photo-luminescent properties of the ligands and complexes are also discussed.

1. Introduction

Metal containing liquid crystals called as metallomesogens have received a lot of attention in the last three decades due to its importance in the basic liquid crystals research as well as its potential utility in industrial, chemical, medical, and sensor applications [1–13]. The nature of metal plays an important role to influence the mesomorphic properties of the organic ligand to which it coordinates. The importance of Schiff bases viz., N-(4-n-alkoxysalicylidene)-4′-n-alkyl(oxy)anilines lies in their rich mesomorphism at ambient temperatures and as well as their suitability for extension with many functional groups [14–16]. Extensive studies are carried out on metallomesogens of d-block elements coordinated to N-(4-n-alkoxysalicylidene)-4′-n-alkyl(oxy)anilines because of the ease of synthesis, stability of the complexes and rich variety of mesophases [10–13]. The incorporation of metal ion with unpaired electrons in these Schiff base ligands can lead to the formation of paramagnetic liquid crystalline (LC) materials. The alignment of paramagnetic LCs possessing large magnetic anisotropy can be realized by small magnetic field strengths. Hence the coordination of paramagnetic lanthanide ions with N-(4-n-alkoxysalicylidene)-4′-n-alkyl(oxy)anilines can generate low molar mass magnetic liquid crystals which possess large magnetic anisotropy. However related studies of the f-block lanthanide ion complexes are relatively limited to N-(4-n-alkoxysalicylidene)-n-alkylamines, **L1-L4** coordinated to lanthanide ions, as shown in Fig. 1 [14–17] apart from few examples of rare-earth containing metallomesogens with other ligands. The first calamitic bidentate salicylideneimine nO(OH)m_{ali}, possessing N-aliphatic moiety based lanthanide complexes was reported in 1991 [14] and a new nomenclature of lanthanidomesogens had been proposed [18–21]. However the efforts in different laboratories [17] to coordinate f-block metals with the salicylideneimine based ligands with an aryl moiety [14–17] on nitrogen atom of the central bridging imine group have been unsuccessful. The difference in basicity of the nitrogens of N-alkyl and N-aryl imines of the ligand to form a zwitter ion led to the coordination of the zwitter ionic N-alkyl imines only to form the lanthanide complexes, while it is not realized with aromatic imines.

N, N′-aromatic donors shown in Fig. 2 [22] viz., 4,7-disubstituted phenanthroline (**L5** and **L6**), or 4,4′-dimethoxy-2,2′-bipyridine (**L7**) coordination with the lanthanide ions was successful, while diethyl-2,2′-bipyridine-4,4′-dicarboxylate (**L8**) did not participate in coordination. Hence it has been accounted for an electronic destabilization of the ester groups on the aromatic bipyridine core, which is associated with a more flexible conformation with respect to the phenanthroline to make this ligand not compatible for chelation with a lanthanide ion of any size. In fact the influence of the substituents on the basicity and the coordination ability of the N, N′-aromatic ligands, viz., 4,4′-dimethoxy-2,2′-bipyridine, (**L3**) the bipyridine bearing a methoxy group in 4,4′-position, produced high yields of the complexes reflecting the dramatically enhanced activation towards coordination.

---

* Corresponding author. Tel.: +91 9435522541; fax: +91 3842270806.
E-mail address: drnvsrao@gmail.com (N.V.S. Rao).

0022-2860/$ - see front matter © 2011 Elsevier B.V. All rights reserved.
doi:10.1016/j.molstruc.2011.07.010

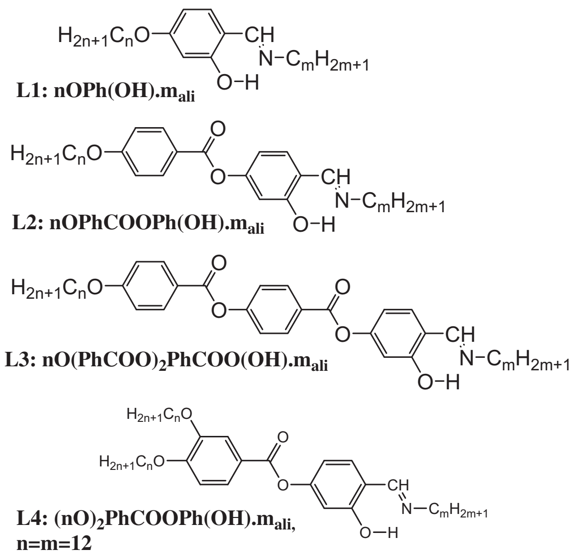

Fig. 1. Molecular structure of Schiff's base ligands studied extensively for complexation [14–17].

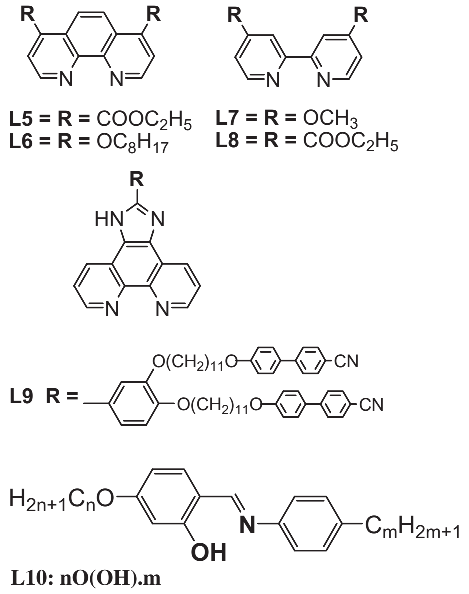

Fig. 2. Molecular structure of N, N′-aromatic donors for complexation.

However modification of the phenanthroline ligand (**L9**) in 5,6-positions fused with a substituted imidazo ring led the realization of nematic phase [23].

Hence the design and synthesis of lanthanide containing liquid crystals viz., salicylideneimine based promesogenic ligands, with a polar group substituted in an aryl moiety on nitrogen atom of the central bridging imine group, to coordinate with f-block metals presents a special experimental challenge. Our previous attempts were successful in reporting the complexation of different lanthanide ions with N-(4-n-alkoxysalicylidene)-4′-n-alkylanilines, **L10** [24,25]. The lanthanide complexes in general exhibited SmA phase but some of them exhibited columnar phases [25,26] depending on the aliphatic chains component in the ligand. In continuation of earlier work we report here the complexation of different lanthanide (III) ions with N-(4-n-hexadecyloxysalicylidene)-4′-substituted-anilines, the substituent being a polar group in N-aryl moiety, characterization of mesomorphism of the ligands as well as complexes and their spectroscopic characteristics. A comparison with complexes of d-block elements is also presented.

2. Results and discussion

The synthesis of ligands viz., N-(4-n-decyloxysalicylidene)-4′-substituted-(methyloxy, chloro and fluoro)-anilines (hereafter abbreviated as 16O(OH)X where X = H, OMe, F, Cl) and their Cu (II) and VO (IV) (*d*-block) complexes and Gd (III) (f-block) complexes as detailed in Scheme 1, was carried out following the procedure described in experimental section. Sm(III) and Pr(III) complexes were also synthesized and characterized by IR, UV–Vis and fluorescence studies.

Elemental analysis of the ligands and copper (II) and oxovanadium (IV) complexes were consistent with their proposed molecular formulas (Table 1). Elemental analysis of lanthanide complexes revealed that the stoichiometry is $\{[Ln(LH)_2L](NO_3)_2\}$, where Ln = Gd, and LH = **2, 3** and **4**. We investigated the ionic conductivity of solutions of the ligand **3** [16O(OH)F], $c = 1.0 \times 10^{-4}$ M and **3-Gd** (Gadolinium complex, $c = 1.0 \times 10^{-3}$ M) in double distilled and dried N,N′-dimethylformamide (DMF). The conductivity values (Table 2) inferred that the ligand is a non-electrolyte. However the **3-Gd**, (Gd complex) is a 2:1 electrolyte with the two nitrate ions participation from outer coordination sphere [27] confirming the elemental analysis data. The room temperature infrared spectra of the ligands **1, 2, 3** and **4** exhibited characteristic bands (ν(C=N)) at 1622–1627 cm^{-1}. The C=N stretching vibration is shifted to lower frequencies for the copper (II) (1608 cm^{-1}) and oxovanadium (IV) (1608–1610 cm^{-1}) complexes compared to that of free ligands. This reflects the azomethine N atom is involved in metal-nitrogen bond formation. The oxovanadium (IV) complexes exhibit a stretching band at around 966–987 cm^{-1} assigned to ν(V—O) suggesting that these complexes have a monomeric structure [28–31].

However the infrared spectra of lanthanide (III) complexes exhibited characteristic C=N stretching vibration (ν(C=N)) at ~1640 ± 5 cm^{-1} and 1616–1622 cm^{-1} (Table 1) for the complexes (Representative IR spectra of the complex **2-Gd** and **3-Gd** are shown in Fig. 3.), apart from the characteristic bands of aromatic ring (C=C), Ar(C—H), CH_3, and CH_2 vibrations. These two bands confirm two types of coordination one through the oxygen atom and another through the nitrogen atom. The band at ~1616–1622 cm^{-1} reflects the participation of azomethine N atom in metal-nitrogen bond formation in the case of toluidine (**2-Gd**) and chloro complexes (**4-Gd**). However the absence of C=N stretching vibration for fluoro complex **3-Gd** at ~1620 cm^{-1} reflects the absence of metal-nitrogen coordination bond formation. The weak O—H stretching vibration of the ligand at 2870–2850 cm^{-1}, is overlapped by the CH modes in the lanthanide complexes reflecting the N—H vibration of the protonated nitrogen atom in $C{=}N^{+}H$ as well as the participation of hydrogen atom in the intramolecular hydrogen bonding with the phenolic oxygen atom as reported earlier [32]. This abnormal behavior may be due to coordination of the metal through O-atom of the ligand only, the proton of the O-atom migrate to the N-atom of the imine moiety which may -lead to formation of zwitter ion ($C{=}N^{+}$—H) of ligand. The observed vibrations of two bands at 1635–1645 cm^{-1} and ~1620 cm^{-1} for the complex $Gd[(L^4H)_2(L)]\cdot(NO_3)_2$, are due to two types of CH=N stretching and compression vibrations. One of these is the elongated stretching viz., exactly opposite with an increase in the imine **C=N** stretching vibration of the complex (at 1635–1645 cm^{-1}) in the infrared spectra when compared to the stretching vibration in the free Schiff base ligand, while the other one is a compressed imine bond appearing at a lower value of 1620 cm^{-1}. The vibration at higher

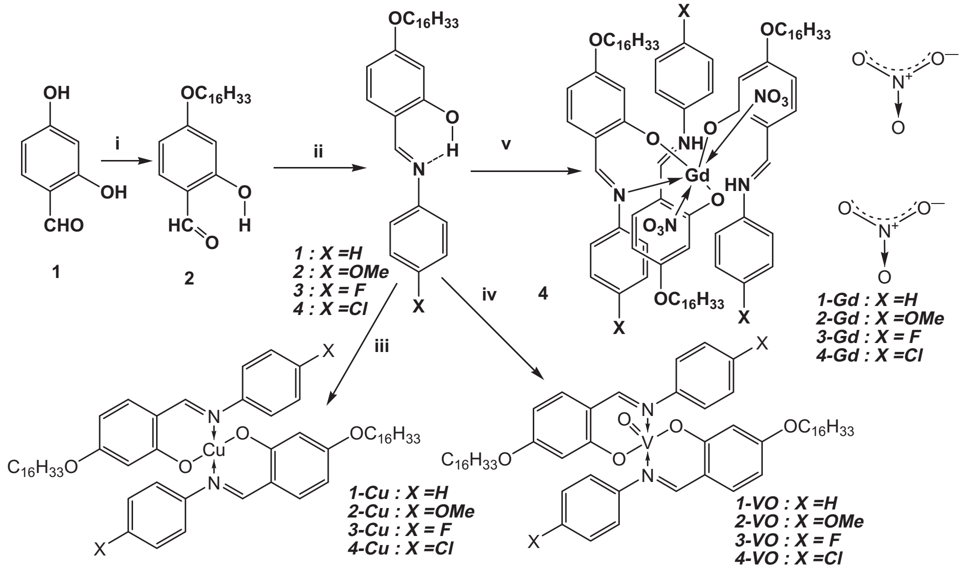

Scheme 1. $C_{16}H_{33}Br$, $KHCO_3$, KI, dry acetone, reflux, 40 h ii. 1 = aniline, 2 = 4-Anisidine, 3 = 4-fluoroaniline, 4 = 4-chloroaniline glacial AcOH, absolute EtOH, Reflux, 4 h iii. $Cu(OAc)_2.H_2O$, EtOH; iv. $VOSO_4.5H_2O$, MeOH, TEA; v. $Gd(NO_3)_3$; Acetonitrile, Reflux, 4 h. For the sake of clarity the coordination of oxygen atoms of nitrate ion is shown through nitrate ions.

Table 1
Elemental analysis data (calculated values in parentheses) and yields of the complexes.

Compound	Molecular formula	C (%)	H (%)	N (%)	Yield (%)	IR data (cm^{-1})
2	$C_{30}H_{45}NO_3$	77.25 (77.04)	9.59 (9.70)	3.09 (2.99)	71	1627
2-Cu	$C_{60}H_{88}CuN_2O_6$	72.55 (72.29)	8.76 (8.90)	2.67 (2.81)	65	1608
2-VO	$C_{60}H_{88}N_2O_7V$	72.14 (72.04)	8.65 (8.87)	2.65 (2.80)	58	1608, 987
2-Gd	$C_{90}H_{134}GdN_5O_{15}$	65.21 (64.22)	7.88 (8.02)	4.39 (4.16)	45	1641,1622
3	$C_{29}H_{42}FNO_2$	76.29 (76.44)	9.19 (9.29)	2.99 (3.07)	74	1625
3-Cu	$C_{58}H_{82}F_2CuN_2O_4$	71.15 (71.61)	8.39 (8.50)	3.01 (2.88)	71	1608
3-VO	$C_{58}H_{82}F_2N_2O_5V$	71.35 (71.36)	8.58 (8.47)	2.65 (2.87)	67	1608, 970
3-Gd	$C_{90}H_{125}F_3GdN_5O_{12}$	62.42 (63.44)	7.21 (7.65)	4.01 (4.25)	42	1645
4	$C_{29}H_{42}ClNO_2$	73.98 (73.78)	8.91 (8.97)	2.88 (2.97)	65	1627
4-Cu	$C_{58}H_{82}Cl_2CuN_2O_4$	69.65 (69.26)	8.29 (8.22)	2.55 (2.79)	61	1608
4-VO	$C_{58}H_{82}Cl_2N_2O_5V$	69.43 (69.03)	8.25 (8.19)	2.59 (2.78)	55	1610, 966
4-Gd	$C_{90}H_{125}Cl_3GdN_5O_{12}$	62.55 (61.59)	7.65 (7.43)	4.31 (4.13)	42	1635, 1620

Table 2
Electrical conductivity of the compound 3, its Gd(III) complex and $Gd(III)NO_3 \cdot 6H_2O$. Concentration is 1×10^{-3} M.

	Molar conductivity (ohm^{-1} cm^2 mol^{-1})		
Compound	N,N′-Dimethylformamide	Ethanol	Acetonitrile
3: 16O(OH)F :L^3H	15	15	9
3-Gd: $[Gd(L^3H)_2L^3](NO_3)_2$	185	92	165
$Gd(NO)_3.6H_2O$	205	83	30

frequency (1635–1645 cm^{-1}) is due to the complexation of oxygen atom with the rare earth ion. This is exactly opposite to the observation of imine **C**=**N** stretching vibration of the copper (II) and VO complexes of **2** and **4** $[Cu(L^4)_2$ at 1608–1610 $cm^{-1}]$ in the infrared spectra which is lower than the imine **C**=**N** stretching vibration of the free ligand L^4H (1627 cm^{-1}), indicating a decrease in strength of the double bond character of **C**=**N** bond. Hence the lower value of 1620 cm^{-1} clearly indicated similar type of coordination of the complexation as in copper complexes which take place through the deprotonated phenolic oxygen and azomethine nitrogen atoms. The phenolic C—O stretching vibration, which is observed in the Schiff base ligands around 1290 cm^{-1}, overlaps in the metal complexes with a vibration due to the nitrate groups. The four bands in the IR spectra of all the lanthanide complexes (only Gd(III) complexes are reported here while Pr(III) and Sm(III) complexes also gave identical spectra) recorded at 1475, 1286, 1122 and 827 cm^{-1} can be assigned to the vibrational modes of the coordinated (C_{2V}) nitrate group reflecting the vibrations of ν_4, ν_1, ν_2, and ν_6 are respectively. Even though it may be assumed that mono dentate nitrate group participates in coordination, the magnitude of splitting in the peak positions of the bands of ν_4 and ν_1 (186 cm^{-1}) characterize the coordination of nitrate group as bidentate rather than mono dentate. The additional bands observed $\sim$1384 cm^{-1} suggests the presence of non-coordinated nitrate groups present in the complex.

3. Thermal behavior: DSC and thermal microscopy

3.1. Mesomorphic behavior of ligands

The polarized optical microscopy was performed to confirm the transition temperatures obtained by DSC studies and to find out

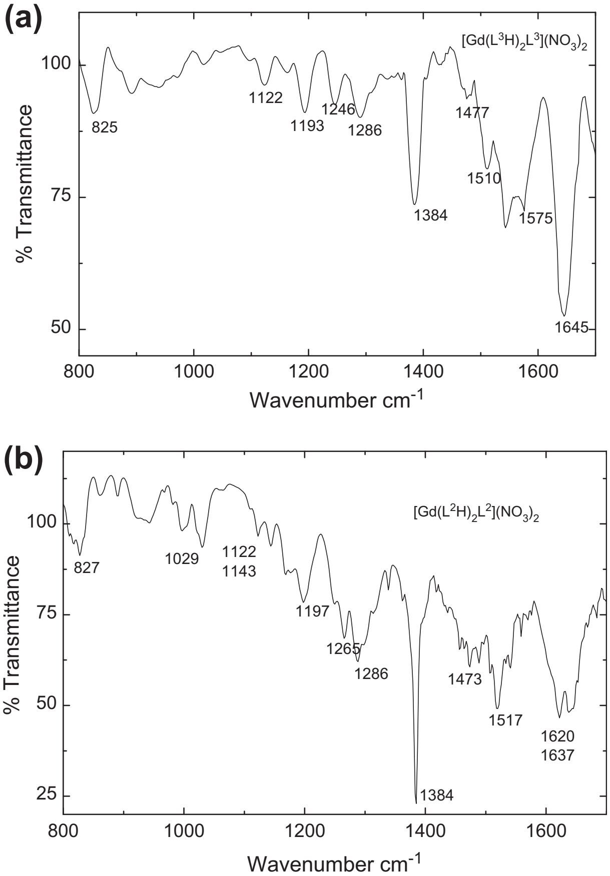

Fig. 3. FTIR spectra of gadolinium (III) complexes of (a) fluoro and (b) methoxy homologs.

the type of liquid crystalline phases present in the studied materials. The liquid crystalline phases, phase transition temperatures, enthalpy and entropy associated with the phase transitions of the ligands and complexes are summarized in Table 3. All the compounds exhibited strong birefringence and fluidity in the temperature range characteristic of mesomorphic behavior between the endothermic or exothermic peaks recorded in DSC thermograms in the heating or cooling cycle respectively. All the ligands exhibit mesomorphism. The compound **1** without any substituent on N-aryl moiety exhibited focal conic fan texture of SmA phase of 0.1 °C. The compound 16O(OH)OMe (**2**) with methoxy group exhibit schlieren texture characteristic of nematic phase (Fig. 4a) while the other two compounds **3** and **4** with a polar substituent (F or Cl respectively) displayed focal conic fan texture characteristic of SmA phase (Fig. 4b,c). The observed mesophase thermal range (ΔT) is 15 °C for 16O(OH)OMe (**2**), 2.3 °C and 34 °C in case of fluoro (**3**) and chloro (**4**) homologs respectively. A representative DSC spectrum of fluoro homolog **3** is displayed in Fig. 5. In a previous report [33–35] on lower homologs of similar compounds viz., 7O(OH)X, where X = H, OMe, F and Cl, 7O(OH)H do not exhibit LC behavior while OMe ($\Delta T \sim 16.9$ °C) exhibits nematic phase, fluoro ($\Delta T \sim 0.5$ °C) and chloro ($\Delta T \sim 50$ °C) homologs exhibit SmA phases. A comparison of transition temperatures between the two homologs (Table 4) revealed the increase in melting/crystallization temperatures. The increase in thermal ranges can be explained as follows.

The thermal stability of the mesophase in these compounds is determined by the anisotropy of the contribution of the polarizability of X, the electronic structure of the N-phenyl moiety under the influence of the substituent inductive and resonance contributions and the associated change in the geometric anisotropy of the molecule. The contribution of substituent polarizability to the total polarizability and polarity of the molecule and the changes induced by the substituent X in the π-conjugation of —CH=N—C_6H_4X fragment as well as the conformation of the molecule determine the thermal stability of the compounds. The methoxy group in N-phenyl moiety with stronger donor properties reduces the effect of π-conjugation of —CH=N—C_6H_4X which is further augmented by the intramolecular H-bonding manifested between the proton of ortho-hydroxyl group in aldehyde moiety and the lone pair of the electrons on the nitrogen atom in azomethine unit. Both these effects contribute to increased planar conformation of the molecule in these compounds in comparison to the noncoplanarity of the phenyl rings on both sides of azomethine linkage in Schiff bases. Hence the apparent stronger dispersion attraction between the planar molecules is reflected in the increase of crystal-mesophase transition temperature when H is replaced by methoxy group.

3.2. Mesomorphic behavior of complexes

All the complexes exhibit smectic A phase while an additional smectic E phase is exhibited by the Cu(II) complexes of fluoro and chloro compounds and all the Gd(III) complexes. The characteristic textures exhibited by the complexes of compounds **2**, **3** and **4** are displayed in Figs. 6–8 respectively. The optical texture of SmE phase with striations across the fans can be seen in for Gd(III) complexes (Figs. 6d and 7d) and for Cu(II) complexes (Fig. 8b). In an earlier report Galyametdinov et al. [35] observed an increase in mesomorphic range of fluoro homolog [N-(4-n-heptyloxysalicylidene)-4′-fluoroaniline] on complexation while a substantial decrease in mesomorphic range of chloro and methoxy homologs. However, in the present work with the increase in carbon chain length from C_7 to C_{16}, enhanced width of mesomorphic range (Table 4) in all the complexes of Cu(II), VO(IV) and Gd(III) than that of the ligands is observed. Hence we rationalize that competing influence between the alkyl chain length and electronic nature of the substituent plays an important role in the mesomorphism of these complexes.

The differential scanning spectra of the fluoro complexes viz., **3-Cu**, **3-VO** and **3-Gd** is displayed in Fig. 9a–c respectively. The mesomorphic thermal range increased from 30.1 °C for copper complex to 103.3 °C and 138.4 °C for oxovanadium and gadolinium complexes, respectively. The predominant influence of metal ion complexation in the manifestation of mesomorphism of a polar ligand is augmented by the suitable end alkyl chain length to enhance the mesomorphic range. The larger width of mesomorphic range (92–136 °C in cooling cycle) particularly in oxovanadium complexes than the copper complexes is surprising and it may be due to electronic interactions of VO moiety as well as functional groups rather than the steric hindrance of the VO group. In general all the Cu(II), VO(IV) and Gd(III) complexes exhibited focal conic fan texture characterizing the phase as SmA, while the Cu(II) and gadolinium (III) complexes of fluoro and chloro compounds exhibited additional phase texture resembling SmE phase. In contrast to the ligands the complexes exhibit wide mesomorphic ranges. The electronic nature and size of the substituent can also influence the molecular structure of the ligands and complexes and thereby affects mesomorphism. It is apparent from the DSC and POM investigations that the width of the mesomorphic range is substantially influenced by the nature of substituent as well as the metal ion in corresponding complexes. These results are in good agreement with the earlier reported results on similar compounds where the alkyloxy chain is heptyloxy homolog [33]. The only difference is the enantiotropic mesophases are observed with the increase in chain length of salicylidene moiety.

Table 3
Phase transition temperatures, associated enthalpy and entropy changes data for the ligands and complexes.

	Compound	Transition	*T* (°C)	ΔH (kJ mol^{-1})	ΔS (J mol^{-1} K^{-1})	Δ*T* (°C)
1	16O(OH)H = (L^1H)	K-I	79.4	66.1	187.6	
		I-SmA	67.3	22.8	67	0.1
		SmA-K	67.2	34.4	101.1	
1-Cu	$Cu(L^1)_2$	K-I	111.6	60.1	157.1	–
		I-K	77.8	80.2	228.6	
1-VO	$VO(L^1)_2$	K-I	106.6	3.63	9.56	–
		I-K	75.8	2.47	18.5	
2	16O(OH)O1 = (L^2H)	K-N	100.5	62.77	185.3	
		N-I	102.2	1.16	3.09	1.7
		I-N	101.3	1.51	4.03	15.0
		N-K	86.3	58.9	164.0	
2-Cu	$Cu(L^2)_2$	K1-K	118.5	18.9	48.5	
		K-SmA	122.8	47.3	119.5	
		SmA-I	141.8	7.01	16.8	19.0
		I-SmA	141.0	7.42	17.9	60.2
		SmA-K	80.8	54.9	155.3	
2-VO	$VO(L^2)_2$	K-SmA	99.3	79.3	213.1	
		SmA-I	195.0	5.64	12.0	95.7
		I-SmA	189.1	3.54	7.66	136.0
		SmA-K	53.02	13.3	40.8	
2-Gd	$[Gd(L^2H)_2L^2](NO_3)_2$	K-SmE	107.7	9.9	26.1	
		SmE-SmA	127.5	12.4	31.1	
		SmA-I	194.3	31.2	66.9	86.6
		I-SmA	192.1*	–		97.1
		SmA-SmE	126.1*	–		
		SmE-K	95.1*	–		
3	16O(OH)F = (L^3H)	K1-K	78.9	0.69	1.96	
		K-I	83.6	56.1	157.4	–
		I-SmA	74.9	3.78	10.8	2.3
		SmA-K	72.6	55.0	159.2	
3-Cu	$Cu(L^3)_2$	K-SmE	119.1	49.5	126.4	
		SmE-SmA	120.8	2.99	7.60	
		SmA-I	125.7	5.05	12.6	6.6
		I-SmA	124.3	5.10	12.8	30.1
		SmA-SmE	97.8	3.32	8.90	
		SmE-K	94.2	60.5	164.7	
3-VO	$VO(L^3)_2$	K-SmA	122.2	76.4	193.4	
		SmA-I	161.9	11.1	25.6	39.7
		I-SmA	160.4	10.8	25.1	103.3
		SmA-K	57.1	21.0	63.8	
3-Gd	$[Gd(L^3H)_2L^3](NO_3)_2$	K-SmE	67.9	12.3	36.2	
		SmE-SmA	139.1*	–	–	
		SmA-I	188.8	10.0	21.7	120.9
		I-SmA	183.5*	–	–	138.4
		SmA-SmE	135.1*	–	–	
		SmE-K	45.1*	–	–	
4	16O(OH)Cl = (L^4H)	K-SmA	87.9	66.9	185.4	
		SmA-I	106.4	5.8	15.2	19.5
		I-SmA	105.9	5.43	14.3	34.0
		SmA-K	71.9	67.7	196.5	
4-Cu	$Cu(L^4)_2$	K-SmE	117.4	36.9	94.6	
		SmE-SmA	172.1	19.1	42.9	
		SmA-I	179.6	7.52	16.6	62.2
		I-SmA	175.6	5.22	11.6	67.6
		SmA-SmE	144.4	22.9	55.0	
		SmE-K	108.0	23.1	60.7	
4-VO	$VO(L^4)_2$	K-SmA	115.5	32.3	83.4	
		SmA-I	144.7	6.40	15.3	29.4
		I-SmA	143.4	5.28	12.7	92.6
		SmA-K	50.8	11.8	36.5	
4-Gd	$[Gd(L^4H)_2L^4](NO_3)_2$	K-SmE	87.5	47.6	132.0	
		SmE-SmA	92.6	2.86	7.8	
		SmA-I	163.0	6.3	14.5	75.5
		I-SmA	161.1*	–	–	
		SmA-SmE	82.5*	–	–	
		SmE-K	45.2*	–	–	

* Indicates the POM observed values.

4. Optical absorption and emission studies

The UV–Visible absorption (Table 5) and fluorescence spectroscopic properties of compound **4** and its complexes in chloroform solution with concentration ($c = 1 \times 10^{-5}$), Fig. 10 (with chloroform as the solvent being chosen to maximize the molecular solubility) were studied to obtain the information regarding absorption and emission maxima, and the Stokes shift of fluorescence. The green

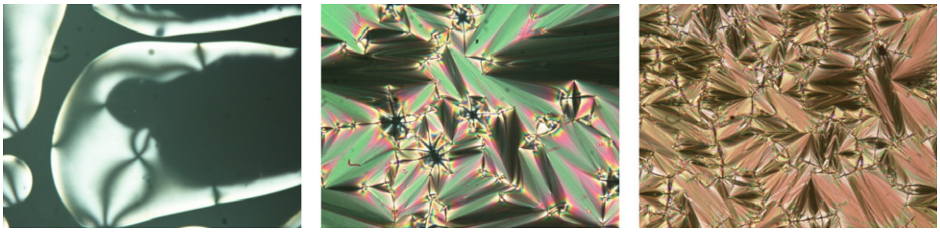

(a) Schlieren texture of nematic phase of **2** at 100.6 ^{0}C

(b) Focal conic texture of SmA phase of **3** at 74 ^{0}C

(c) Focal conic texture of SmA phase of **4** at 105.4 ^{0}C

Fig. 4. (a) Schlieren texture of nematic phase of **2** at 100.6 °C, (b) focal conic texture of SmA phase of **3** at 79 °C, and (c) focal conic texture of SmA phase of **4** at 105.4 °C.

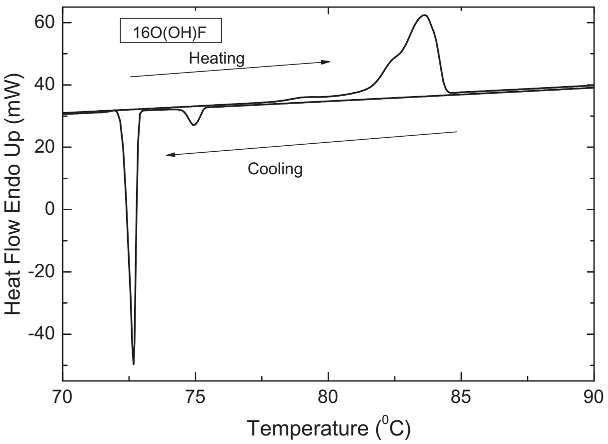

Fig. 5. DSC spectrum of the compound **3**.

fluorescence of **4-Gd** when exposed to UV light is shown in Fig. 11. The absorption maxima of the lowest optical transition were observed approximately at 342–355 nm for compound 4 (and other ligands as well) (~3.6 eV, ~ε = 80,000–146,000 L mol^{-1} cm^{-1}) with two other maxima in at 245 nm and 300 nm. The extended conjugated π-system is reflected in the electronic absorption spectrum. The electronic properties of these systems are dominated by the donor–acceptor-substituted organic chromophore ligand bands with a noticeable shift for the d-block complexes. However no noticeable shift to lower or higher energy levels for the lanthanide complexes is observed indicating the absence of crystal field effect upon the inter-electronic repulsion between the *4f* electrons of the metal ion. These absorption bands with large molar absorption coefficients reflects the π–π^* transition of the highly π-conjugated system of the ligand surrounding the metal ion core. Luminescence studies of metallomesogens are scanty [36] and luminescent studies on the ligand and complexes were carried out in solution and thin film of the solid phases. The most important features of the photoluminescence emission spectra of the lanthanide metallomesogens and ligands in chloroform solution at different concentrations and in thin solid film are the large Stokes shifted emission of ~174 nm for **4-Gd** complex and ~122–129 nm (Fig. 10) and broad emission band with maxima in the vicinity of ~520 nm and ~471 nm for **4-Gd** and **4-Pr** complexes respectively. The Stokes shift, which reflects the structural relaxation of the excited molecule, is in the range reported for other metallomesogens [37–39] but significantly larger than the reported push–pull systems [40–44] exhibiting liquid crystal behavior, confirmed the molecular conformational changes upon excitation. Hence it can be assigned to the ligand–ligand charge transfer transition due to the presence of phenyl rings in the ligands and also indicative of phosphorescence. Further studies are in progress to change the design of the ligand to promote metal centered absorption and emission.

5. Conclusions

The synthesis of *d*- and f-block metal complexes of N-(4-n-hexadecyloxysalicylidene)-4′-substituted anilines, with the polar substituents (Cl and F), exhibiting mesomorphism had been successfully achieved. Proper choice of end alkyl chain length can influence the manifestation of mesomorphism in ligands as well as their complexes. Hence competing influence between the alkyl chain length and electronic nature of the substituent plays an important role in the mesomorphism of these complexes. In particular the special experimental challenge of synthesis of lanthanide containing liquid crystals viz., salicylideneimine based promesogenic ligands, with *a polar group substituted in an aryl moiety on nitrogen atom of the central bridging imine group* is fulfilled. These complexes possess large thermotropic mesomorphic range exhibiting SmA and SmE phases. The major advantage of Lanthanide containing metallomesogens is intense luminescence characteristics as well as large mesomorphic range close to ambient temperature. The studies on magnetic anisotropy of these complexes is still to be explored and further work is in progress to synthesize stable room temperature lanthanidomesogens exhibiting nematic and smectic phases by suitable changes in the end alkyl chains, substituents in the aromatic core and counter-ions.

Table 4
Comparison of transition temperatures and mesomorphic range in °C of ligands and complexes.

		H	OMe	Me	F	Cl
Melting point of 7O(OH)X	Heating	50.9	90.0	64.9	73.0	72.0
Melting point/crystallization of 16O(OH)X	Heating	79.4	100.5	84.6	83.6	87.9
	Cooling	–	102.2	84.6	83.6	106.4
ΔT of 16O(OH)X		0.1	15.0	1.5	2.3	34.0
Cu(II) complexes of 16O(OH)X		–	60.2	3.7	30.1	67.6
VO(IV) complexes of 16O(OH)X		–	136.0	33.1	103.3	92.6

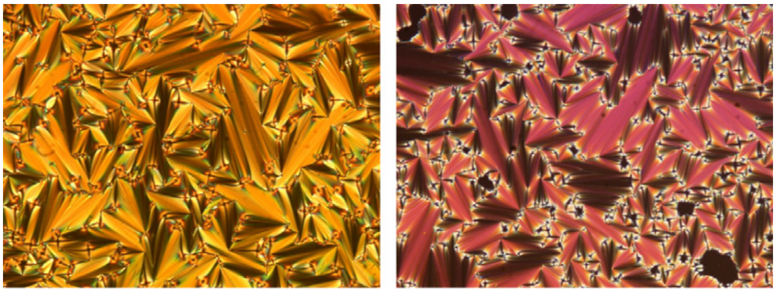

(a) SmA phase texture of **2-Cu**, $[L^2]_2Cu$, at 137.2 ^{0}C

(b) SmA phase texture of **2-VO**, $[L^2]_2VO$ at 127.2 ^{0}C

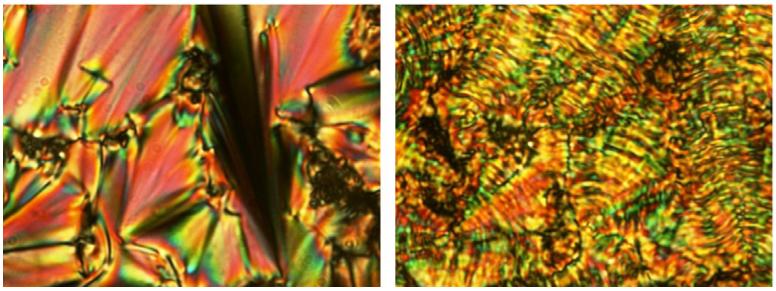

(c) SmA phase texture of **2-Gd** at 192 ^{0}C

(d) SmE phase texture of **2-Gd** at 125 ^{0}C

Fig. 6. Focal conic fan textures exhibited by complexes of compound **2**: **2-Cu, 2-VO and 2-Gd**.

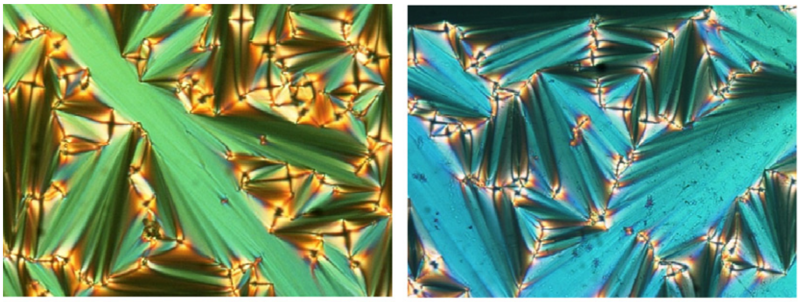

(a) SmA phase texture of **3-Cu**, $[L^3]_2Cu$ 119 ^{0}C

(b) SmA phase texture of **3-VO**, $[L^3]_2VO$ 151.9 ^{0}C

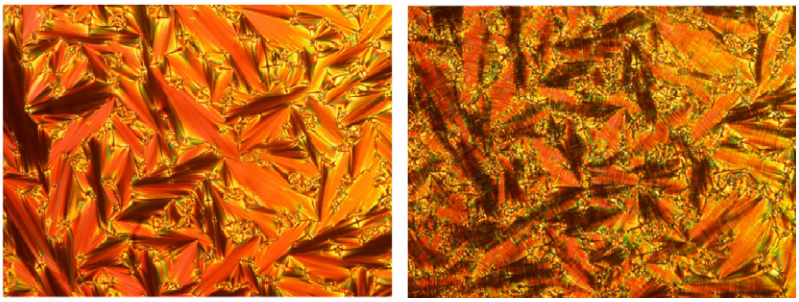

(c) SmA phase texture of **3-Gd**, $[Gd(L^3H)_2L^3](NO_3)_2$ 182.6 ^{0}C

(d) SmE phase texture of **3-Gd**, $[Gd(L^3H)_2L^3](NO_3)_2$ 130 ^{0}C

Fig. 7. Focal conic fan textures exhibited by complexes of compound **3**: **3-Cu, 3-VO and 3-Gd**.

6. Experimental

All the chemicals were procured from M/s Alfa Aesar, Tokyo Kasei Kogyo Co. Ltd. or Lancaster chemicals, Sigma–Aldrich Chemicals. The solvents and reagents are of AR grade and were distilled and dried before use. Microanalysis of C, H and N elements were determined on Carlo-Erba 1106 elemental analyzer. IR spectra were recorded on a Shimadju FT-IR-prestige-21spectrometer $(\nu_{\max}$

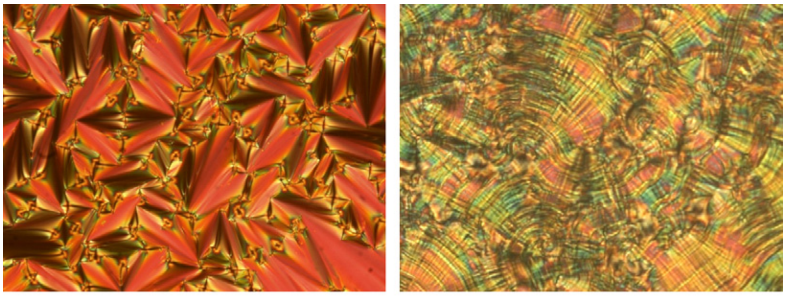

(a) SmA phase texture of **4-Cu**, $[L^4]_2Cu$ 172 ^0C

(b) SmE phase texture of **4-Cu**, $[L^4]_2Cu$ 141 ^0C

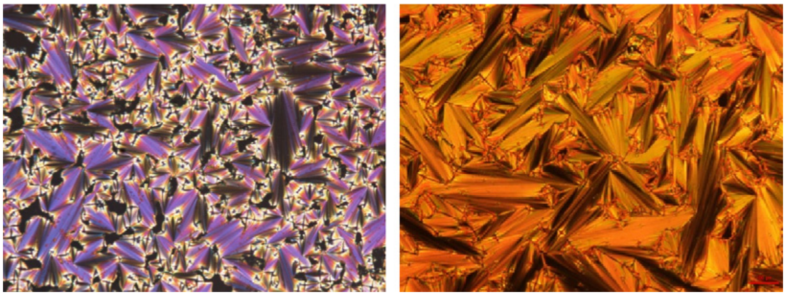

(c) SmA phase texture of **4-VO**, $[L^4]_2VO$ 126.4 ^0C

(d) SmA phase texture of **4-Gd** $[Gd(L^4H)_2L^4](NO_3)_2$ 132 ^0C

Fig. 8. Focal conic fan textures exhibited by complexes of compound **4: 4-Cu, 4-VO and 4-Gd**.

in cm^{-1}) over the 400–4000 cm^{-1} spectral range in KBr pellets. The ^1H NMR spectra of all the organic ligands were recorded in $CDCl_3$ solution on a JEOL AL300 FTNMR spectrometer. Conductivity measurements were performed in DMF solution 10^{-3} M on a Systronics CM304 conductivity meter. Chemical shifts are reported in parts per million (δ) relative to tetramethylsilane (TMS) as internal standard. The phase transition temperatures and associated enthalpies were recorded with a heating and cooling rate of 5 °C/min using differential scanning calorimetry (DSC) (Perkin-Elmer Pyris-1 system). The DSC apparatus was calibrated with indium (156.6 °C, 28.4 J/g) and tin (232.1 °C, 60.5 J/g). The liquid crystalline properties of the different phases exhibited by the ligands and complexes were observed and characterized using polarizing microscope (Nikon optiphot-2-pol attached with hot and cold stage HCS302, with STC200 temperature controller configured for HCS302 from INSTEC Inc. USA). UV visible absorption spectra of the compounds in $CHCl_3$ at different concentrations were recorded on a Shimadzu UV-1601PC spectrophotometer (λ_{max} in nm). Fluorescence spectra were recorded with a Shimadju RF-5301PC spectroflouorometer with 150 W xenon lamp as the excitation source.

7. Preparation of ligands and metal complexes

Synthesis of the Schiff bases: The free ligands were synthesized following a well known procedure [45–48] by refluxing a mixture of ethanolic solution of 1 mmol of the 4-n-hexadecyloxysalicylaldehyde with 1 mmol of appropriate amine and few drops of glacial acetic acid as catalyst for 3 h. The precipitated product was purified by repeated recrystallization from absolute ethanol till constant clearing temperatures are achieved (yield 65–75%).

Synthesis of aldehyde: 4-n-hexadecyloxy salicylaldehyde was synthesized as described earlier [46–48] using modified Williamson's method by refluxing 1 mmol of 1-bromohexadecane and 1 mmol of 4-hydroxysalicylaldehyde in the presence of $KHCO_3$ (1 mmol) as base in dry acetone. The product was purified by column chromatography using hexane as eluent.

Preparation of the metal complexes: The synthesis of copper (II) complexes was carried out by refluxing the mixture consisting of slowly added ethanolic copper (II) acetate $[Cu(OAc)_2 \cdot H_2O]$ (1 mmol) solution (20 ml) to a hot solution of the appropriate ethanolic imine (2 mmol) solution (~50 ml) for 2 h. The solution was cooled to room temperature and filtered to yield the brown copper (II) complexes which were subsequently recrystallized from a mixture of ethyl acetate and ethanol.

Oxovanadium (IV) complexes were prepared by refluxing the mixture consisting of slowly added 20 ml of methanolic vanadium (IV) oxide sulfate ($VOS0_4{\cdot}5H_2O$) (1 mmol) solution to a hot solution of the appropriate imine (2 mmol) in methanol (50 ml) in the presence of triethylamine for 4 h. The solution was cooled to room temperature and filtered to yield the green oxovanadium (IV) complexes which were subsequently recrystallized from a mixture of ethyl acetate and ethanol.

Gadolinium (III) complexes were synthesized by refluxing by refluxing the mixture consisting of slowly added gadolinium (III) nitrate $[Gd(NO_3)_3]$ (1 mmol) solution in acetonitrile (20 ml) to a hot solution of the appropriate imine (3 mmol) solution in acetonitrile (~50 ml) for 4 h. The solution was filtered, when it is hot to avoid the impurity of unreacted ligand and to yield the pale yellow precipitate of gadolinium (III) complexes which were washed repeatedly with acetonitrile. The precipitate was dried for further analysis.

Acknowledgement

The authors acknowledge the financial assistance from DAE, DST and UGC.

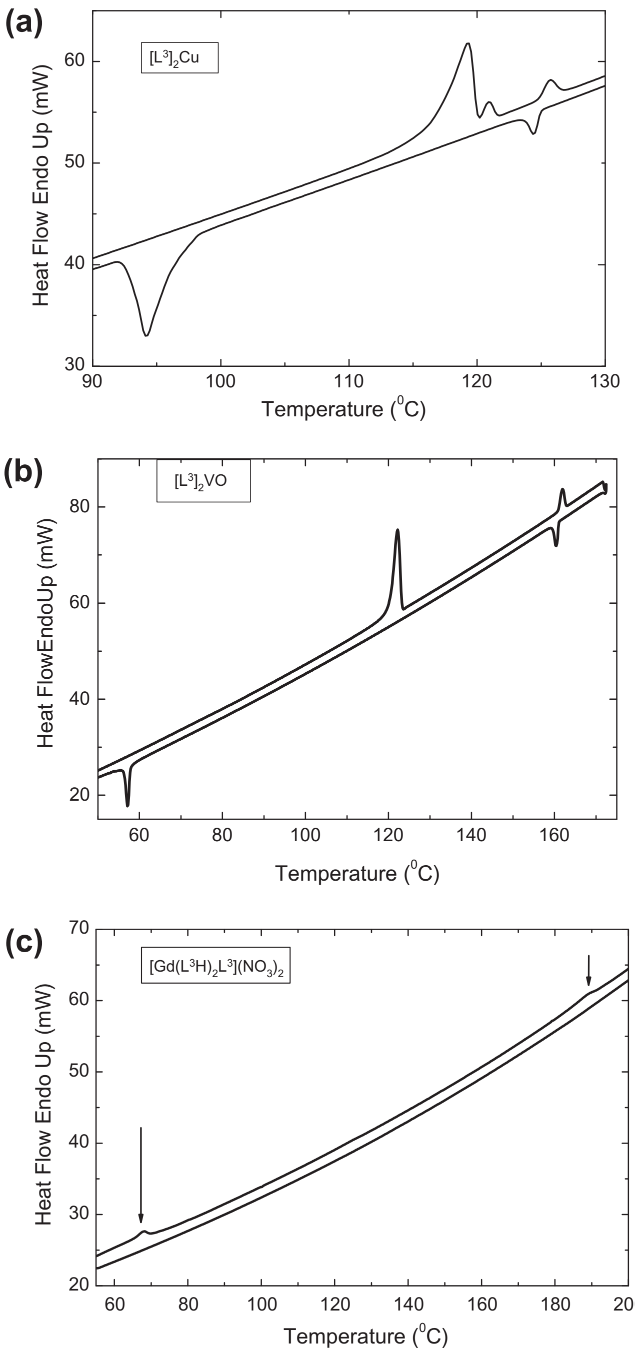

Fig. 9. (a) DSC spectrum of the compound **3-Cu**, (b) DSC spectrum of the compound **3-VO**, (c) DSC spectrum of the compound **3-Gd**.

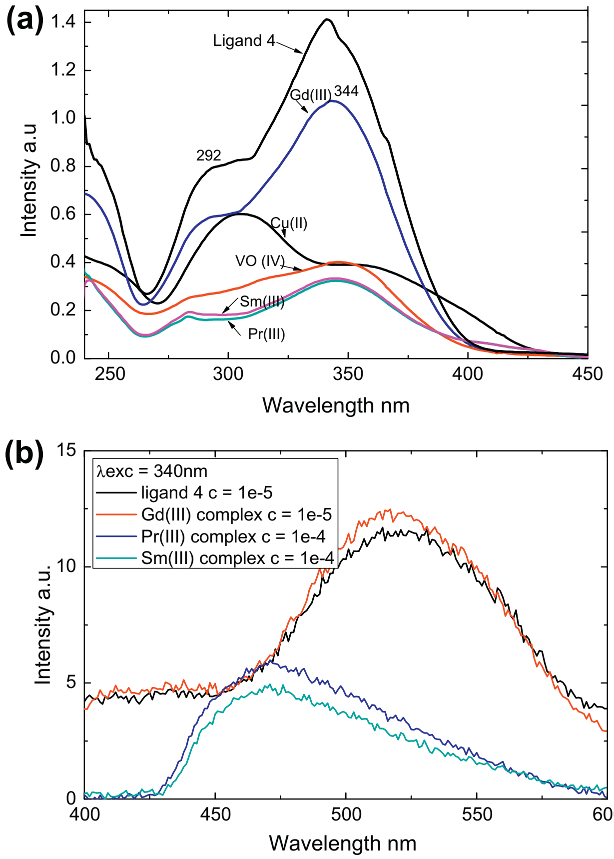

Fig. 10. (a) UV–Visible spectra of compound **4** and its Cu(II), VO(IV) and lanthanide complexes. (b) Fluorescence spectra of compound **4** and lanthanide complexes. Conc = 1 × 10^{-5} M.

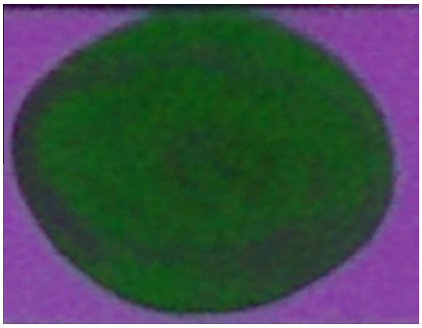

Fig. 11. Fluorescent image of **4-Gd** in solid state.

Table 5
UV–Visible data for the compound **4** and its complexes. (First row indicates the absorption wavelength in nm and second row indicates the molar extinction coefficient L mol^{-1} cm^{-1}.)

4	4-Cu	4-VO	4-Gd	4-Sm	4-Pr
245		234	237	241	
82,000		34,300	68,600	32,600	
300	302	284	292	282	283
81,300	59,900	25,500	58,700	18,800	17,500
		312			
		32,900			
345	355	346	344	344	343
133,800	39,100	39,900	107,300	33,400	32,400

References

[1] J.L. Serrano (Ed.), Metallomesogens, Synthesis, Properties and Applications, VCH, Weinheim, Germany, 1996.
[2] A.M. Giroud-Godquin, Metal-containing liquid crystals, in: D. Demus, J.W. Goodby, G.W. Gray, H.W. Spiess, V. Vill (Eds.), Handbook of Liquid Crystals, vol. IIB, Wiley-VCH, Weinheim, Germany, 1998, pp. 901–932.
[3] A.M. Giroud-Godquin, P.M. Maitlis, Angew. Chem. Int. Edit. Engl. 30 (1991) 375.
[4] P. Espinet, M.A. Esteruelas, L.A. Oro, J.L. Serrano, E. Sola, Coordin. Chem. Rev. 117 (1992) 215.
[5] D.W. Bruce, in: D.W. Bruce, D. O'Hare (Eds.), Inorganic Materials, second ed., Wiley, Chichester, 1996, pp. 405–490, (Chapter 8).
[6] D.W. Bruce, J. Chem. Soc. Dalton Trans. (1993) 2983.
[7] A.P. Polishchuk, T.V. Timofeeva, Russ. Chem. Rev. 62 (1993) 291.
[8] S.A. Hudson, P.M. Maitlis, Chem. Rev. 93 (1993) 861.
[9] L. Oriol, J.L. Serrano, Adv. Mater. 7 (1995) 348.
[10] N. Hoshino, Coordin. Chem. Rev. 174 (1998) 77.
[11] B. Donnio, D.W. Bruce, Struct. Bond. 95 (1999) 193–247.
[12] B. Donnio, D. Guillon, R. Deschenaux, D.W. Bruce, in: J.A. McCleverty, T.J. Meyer (Eds.), Comprehensive Coordination Chemistry II: From Biology to Nanotechnology, vol. 7, Elsevier, Oxford, UK, 2003, pp. 357–627.
[13] D.W. Bruce, R. Deschenaux, B. Donnio, D. Guillon, in: R.H. Crabtree, D.M.P. Mingos (Eds.), Comprehensive Organometallic Chemistry III, vol. 12, Elsevier, Oxford, UK, 2007, pp. 195–293. Chapter 12.05.
[14] Y.G. Galyametdinov, G.I. Ivanova, I.V. Ovchinnikov, Bull. Acad. Sci. USSR Div. Chem. Sci. 40 (1991) 1109.
[15] K. Binnemans, C. Gorller-Walrand, Chem. Rev. 102 (2002) 2303.
[16] K. Binnemans, Yu.G. Galyametdinov, R. Van Deun, D.W. Bruce, S.R. Collinson, A.P. Polishchuk, I. Bikchantaev, W. Haase, A.V. Prosvirin, L. Tinchurina, I. Litvinov, A. Gubajdullin, A. Rakhmatullin, K. Uytterhoeven, L. Van Meervelt, J. Am. Chem. Soc. 122 (2000) 4335.
[17] K. Binnemans, D.W. Bruce, S.R. Collinson, R. Van Deun, Yu.G. Galyametdinov, F. Martin, Phil. Trans. Roy. Soc. Lond. A357 (1999) 3063.
[18] E. Terazzi, S. Suarez, S. Torelli, H. Nozary, D. Imbert, O. Mamula, J.P. Rivera, E. Guillet, J.M. Benech, G. Bernardinelli, R. Scopelliti, B. Donnio, D. Guillon, J.C.G. Bunzli, C. Piguet, Adv. Funct. Mater. 16 (2006) 157.
[19] C. Piguet, J.C.G. Bunzli, Chem. Soc. Rev. 28 (1999) 347.
[20] J.C.G. Bunzli, Acc. Chem. Res. 39 (2006) 53.
[21] J.C.G. Bunzli, C. Piguet, Chem. Rev. 102 (2002) 1897;
J.C.G. Bunzli, C. Piguet, Chem. Soc. Rev. 34 (2005) 1048.
[22] A. Bellusci, G. Barberio, A. Crispini, M. Ghedini, M. La Deda, D. Pucci, Inorg. Chem. 44 (2005) 1818.
[23] T. Cardinaels, K. Driesen, I.N.P. Vogt, B. Heinrich, C. Bourgogne, D. Guillon, B. Donnio, K. Binnemans, Chem. Mater. 17 (2005) 6589.
[24] N.V.S. Rao, M.K. Paul, T.R. Rao, A. Prasad, Liq. Cryst. 29 (2002) 1243.
[25] N.V.S. Rao, T.D. Choudhury, R. Deb, M.K. Paul, T.R. Rao, T. Francis, I.I. Smalyukh, Liq. Cryst. 37 (2010) 1393.
[26] F. Martin, S.R. Collinson, D.W. Bruce, Liq. Cryst. 27 (2000) 859.
[27] W.J. Geary, Coordin. Chem. Rev. 7 (1971) 81.
[28] R.L. Farmer, F.L. Urbach, Inorg. Chem. 13 (1974) 587.
[29] M. Pasquali, F. Marchetti, S. Merlino, J. Chem. Soc., Dalton Trans. (1977) 139.
[30] A. Serrete, J. Carroll, T.M. Swager, J. Am. Chem. Soc. 114 (1992) 1887.
[31] E. Campillos, M. Marcos, A. Omenat, J.L. Serrano, J. Mater. Chem. 6 (1996) 349.
[32] S. Kumari, A.K. Singh, K.R. Kumar, B. Sridhar, T.R. Rao, Inorg. Chim. Acta 362 (2009) 4205.
[33] I.V. Ovchinnikov, Y.G. Galyametdinov, G.I. Ivanova, L.M. Yagfarova, Dokl. Akad. Nauk. SSSR 276 (1984) 126.
[34] Y.G. Galyametdinov, G.I. Ivanova, Izv. Akad. Nauk. SSSR, Ser. Khim. 9 (1989) 1997.
[35] Y.G. Galyametdinov, G.I. Ivanova, Izv. Akad. Nauk. SSSR, Ser. Khim. 12 (1989) 2833.
[36] K. Binnemans, J. Mater. Chem. 19 (2009) 448.
[37] D. Pucci, G. Barberio, A. Bellusci, A. Crispini, B. Donnio, L. Giorgini, M. Ghedini, M.L. Deda, E.I. Szerb, Chem. Eur. J. 12 (2006) 6738.
[38] R. Bayon, S. Coco, P. Espinet, Chem. Eur. J. 11 (2005) 1079.
[39] J. Arias, M. Bardaji, P. Espinet, Inorg. Chem. 47 (2008) 3559.
[40] H. Gallardo, R. Cristiano, A.A. Vieira, R.A.W. Neves Filho, R.M. Srivastava, I.H. Bechtold, Liq. Cryst. 35 (2008) 857.
[41] A.A. Vieira, R. Cristiano, A.J. Bortoluzzi, H.J. Gallardo, Mol. Struct. 875 (2008) 364.
[42] R.M. Srivastava, R.A.W.N. Filho, R. Schneider, A.A. Vieira, H. Gallardo, Liq. Cryst. 35 (2008) 737.
[43] R. Cristiano, F. Ely, H. Gallardo, Liq. Cryst. 32 (2005) 15.
[44] A.A. Vieira, R. Cristiano, F. Ely, H. Gallardo, Liq. Cryst. 33 (2006) 381.
[45] C.K. Lai, Y. Leu, Liq. Cryst. 25 (1998) 689.
[46] N.V.S. Rao, T.D. Choudhury, M.K. Paul, T. Francis, Liq. Cryst. 36 (Suppl.) (2009) 409.
[47] P. Keller, L. Liebert, Solid State Phys. 14 (1978) 19.
[48] M. Artigas, M. Marcos, E. Melendez, J.L. Serrano, Mol. Cryst. Liq. Cryst. 130 (1985) 337.